Materials Research Letters

ISSN: (Print) 2166-3831 (Online) Journal homepage: http://www.tandfonline.com/loi/tmrl20

Residual stress induced tension-compression asymmetry of gradient nanograined copper

Jianzhou Long, Qingsong Pan, Nairong Tao & Lei Lu

To cite this article: Jianzhou Long, Qingsong Pan, Nairong Tao & Lei Lu (2018) Residual stress induced tension-compression asymmetry of gradient nanograined copper, Materials Research Letters, 6:8, 456-461, DOI: 10.1080/21663831.2018.1478898

To link to this article: https://doi.org/10.1080/21663831.2018.1478898

MATER. RES. LETT.
2018, VOL. 6, NO. 8, 456–461
https://doi.org/10.1080/21663831.2018.1478898

MATERIALS RESEARCH LETTERS
Taylor & Francis
Taylor & Francis Group

ORIGINAL REPORT

Residual stress induced tension-compression asymmetry of gradient nanograined copper

Jianzhou Long[a,b,#], Qingsong Pan[a,#], Nairong Tao[a] and Lei Lu[a]

[a]Shenyang National Laboratory for Materials Science, Institute of Metal Research, Chinese Academy of Sciences, Shenyang, People's Republic of China; [b]University of Chinese Academy of Sciences, Beijing, People's Republic of China

ABSTRACT

The residual stress significantly influences the cyclic stress response of the hierarchical nanostructured materials. An obvious tension-compression asymmetry with minimum stress in compression larger than maximum stress in tension was observed in gradient nanograined (GNG) Cu under strain-controlled high-cycle fatigue tests, which gradually diminished with increasing cycles or after being annealed at a low temperature. The observed asymmetric response is primarily induced by the presence of the residual compressive stress in the GNG surface layer. The longer fatigue life can be achieved in GNG Cu with a higher residual stress, compared to that of annealed GNG Cu.

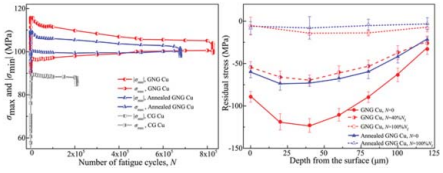

IMPACT STATEMENT

Obvious tension-compression asymmetry was observed in cyclically deformed gradient nanograined Cu under strain control, caused by the residual compressive stress in the GNG surface layer.

ARTICLE HISTORY
Received 22 March 2018

KEYWORDS
Gradient nanograin; cyclic response; tension and compression asymmetry; residual stress

1. Introduction

Gradient nanograined (GNG) metals, as a promising hierarchical structure with grain sizes spatially increasing from nanoscale in surface to coarse grain (CG) in core, have attracted considerable interests, due to their unusual combination of high strength and considerable ductility in tensile tests [1–4]. Their fatigue properties and behaviours under cyclic loading are also very essential, which determine their prospect of engineering application [5]. Recently, studies have shown that the high-cycle fatigue properties (including cyclic stress and fatigue life in S-N curve) of GNG metals under stress-controlled cyclic loading tests are remarkably enhanced, relative to CG counterparts, which are mainly attributed to the presence of high-strength GNG surface layer to suppress crack initiation [6–8]. For instance, abnormal grain coarsening initiates at the subsurface layer of cyclically deformed GNG Cu and with increasing cycles gradually extends to the top surface, where fatigue crack initiates [7,9].

Previous studies showed that the introduced residual stress in sample surface layers can obviously enhance the stress-controlled high-cycle fatigue properties of metals subjected to shot peening and deep rolling [10–13]. In fact, residual stress is also induced in GNG layer during the process of preparing GNG metals via the surface mechanical treatment [8]. However, limited studies showed that with the relaxation of residual stress in GNG 316L stainless steel after annealing treatment, its high-cycle fatigue property is still elevated, which may be closely related with the martensitic transformation in the GNG layer during annealing and enhanced strength [6]. To date, whether the residual stress influences high-cycle fatigue properties and cyclic

CONTACT Lei Lu llu@imr.ac.cn Shenyang National Laboratory for Materials Science, Institute of Metal Research, Chinese Academy of Sciences, Shenyang 110016, People's Republic of China
[#]These authors contributed equally to this work.

Supplemental data for this article can be accessed here. https://doi.org/10.1080/21663831.2018.1478898

deformation behaviour of GNG metals are still an open question.

Without monitoring the plastic strain information, stress-controlled fatigue tests is obviously insufficient to clarify the effect of residual stress on high cycle fatigue properties of GNG metals. Relative to stress control, strain-controlled fatigue tests can provide additional strain information and cyclic strain–stress response, which is essential for an in-depth understanding of cyclic deformation mechanism and structure (including residual stress)-fatigue property relationship of metals [5,14,15]. However, the cyclic stress–strain response of GNG metals in the traditional high-cycle regime is not reported yet.

In this study, cyclic stress–strain responses of GNG Cu and that after short time annealing are assessed via strain-controlled high-cycle fatigue tests. The microstructure and residual stress evolution influencing on high-cycle stress response and fatigue properties of GNG Cu are clarified as well.

2. Experimental

Commercial purity Cu rods with an average grain size of 21 μm and a yield strength of 56 MPa were initially machined into dog-bone-shaped samples with a gauge diameter of 6 mm and a gauge length of 12 mm. Both their gauge sections and arc transitions were then processed by surface mechanical grinding treatment (SMGT) to produce GNG Cu with a gradient nanograined layer, which was described in detail in [1,7]. Besides, one set of GNG Cu samples were annealed at 80°C for 10 min, which was hereafter referred to as annealed GNG Cu.

Symmetric tension-compression fatigue tests of two types GNG Cu were performed in an Instron E10000 fatigue machine under strain control at ambient temperature. A strain extensometer with a gauge length of 10 mm was applied to control the strain amplitude. The applied total strain amplitude ($\Delta\varepsilon_t/2$) was 0.12%, which was approximately equal to the calculated $\Delta\varepsilon_t/2$ value of GNG Cu at the stress amplitude of 140 MPa [7]. A triangle waveform with a frequency of 2 Hz was used. For comparison, CG Cu samples with the same grain size with that of CG core in GNG Cu are cyclically deformed at the same condition.

Cross-sectional microstructures of GNG and annealed GNG Cu before and after fatigue tests were characterized by using the FEI Nova NanoSEM430 scanning electron microscope (SEM) and FEI Tecnai F20 transmission electron microscope (TEM), respectively. A pure Cu layer was firstly electro-deposited onto the surface of GNG samples. Then, cross-sectional SEM and TEM foils were cut parallel to the cyclic loading axis by an electrical spark machine and mechanically ground. SEM foils were electro-polished in an electrolyte of phosphoric acid (25 Vol.%), alcohol (25 Vol.%) and deionized water (50 Vol.%) at 5 V for 30 s while TEM Cu foils were thinned by twin-jet polishing in the same electrolyte at about −10°C. Over 500 grains from numerous TEM images were measured to determine the average grain size in different depth of GNG layer.

Residual stresses (σ_r), along the axial direction in both GNG and annealed GNG Cu with different fatigue cycles were measured by X-ray diffraction (XRD) using classical $2\theta - \sin^2\psi$ method with Cu K_α radiation on {420} plane [16,17], as follows:

$$\sigma_r = \frac{E}{2(1+\nu)}\cos\theta_0\frac{\pi}{180^\circ}\frac{d(2\theta)}{d(\sin^2\psi)}$$

where ψ is the tilting angle of the normal direction of GNG rod sample surface relative to the plane with X-ray source and detector, ranging from 0 to ~43° (see Figures S1 and S2); 2θ and $2\theta_0$ is the Bragg diffraction angle or the position of the selected diffraction peaks [420] of Cu with and without residual stress (Figure S1); E and ν are elastic modulus and Poisson's ratio of Cu (120 GPa and 0.33), respectively. Based on the slope of θ vs $\sin^2\psi$ (Figure S2(b)) and Equation (1), the residual stress can be calculated. To obtain the residual stresses at various depths beneath the surface, iterative electrolytical removal of thin surface layer of both types GNG samples and subsequent XRD measurement were performed.

3. Results and discussion

Cross-sectional SEM images in Figure 1(a) show that a spatially gradient grain size is distributed in GNG Cu after SMGT process. Closer TEM observations indicate that almost equiaxed nano-sized grains (NGs) with an average grain size of 80 ± 10 nm (Figure 1(b)) are formed in the top 20-μm-thick surface layer. In a depth span of 20 to ~220 μm are ultrafine grains (UFGs), with an average grain size of 218 ± 75 nm at depth of 50 μm (Figure 1(c)). For convenience, both NG and UFG layers are hereafter referred to as the GNG layer. Besides, high-density dislocations exist in GNG layer, where most grains are separated by indistinct curved grain boundaries (GBs), indicating that they are in a non-equilibrium state.

Figure 1(d) shows cross-sectional SEM images of annealed GNG Cu: the spatially gradient grain size is still kept, resembling that in the as-SMGTed state (Figure 1(a)). Closer TEM observations reveal that numerous NGs and UFGs in GNG layer still have high-density dislocations, which are separated by curved

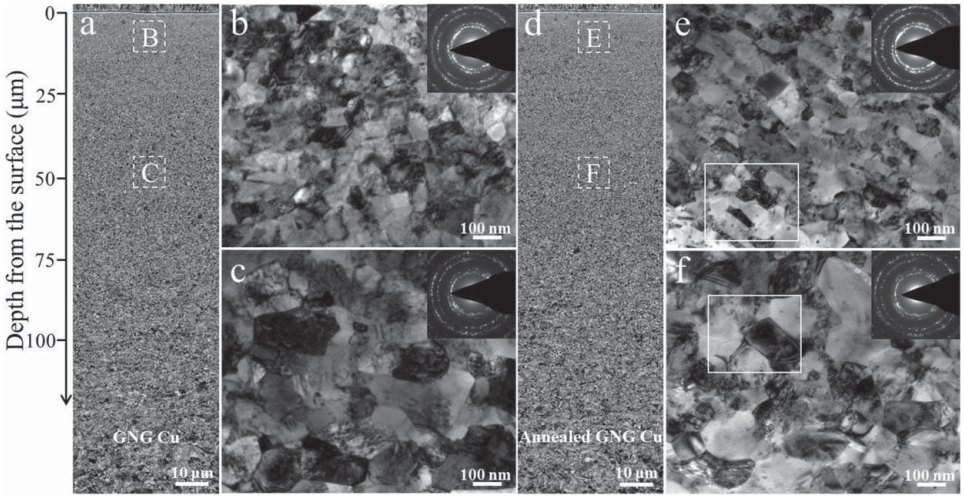

Figure 1. Typical cross-sectional SEM images of GNG Cu (a) in the as-SMGTed state and (d) after annealing treatment. TEM images of GNG Cu at positions B and C indicated in (a) are shown in (b–c) and those of annealed GNG Cu at positions E–F indicated in (d) are shown in (e–f). The insets in (b–c) and (e–f) are SAED patterns.

GBs (Figure 1(e,f)), like that in Figure 1(b,c). Differently, grains in GNG layer become cleaner. GBs become sharper and distinct, as highlighted in Figure 1(e,f). Statistics of grain size distributions showed that the mean average grain sizes at a depth of 20 μm thick and 50 μm in the top surface layer of GNG Cu before and after annealing treatment are nearly the same. The selected-area electron diffraction (SAED) patterns (insets in Figure 1(b, c, e and f)) reveal that these NGs and UFGs are randomly oriented before and after annealing. These results demonstrate that slightly microstructural recovery, instead grain growth, occurred in the GNG layer during low-temperature annealing, indicating that annealed GNG Cu exhibits a similar gradient microstructure but with a relative lower defect density, compared with that in the as-SMGTed state.

Figure 2 shows cyclic stress responses (maximum stress in tension, σ_{max} and minimum stress in compression, σ_{min}) of GNG Cu and annealed GNG Cu cyclically deformed at $\Delta\varepsilon_t/2$ of 0.12%. Note that to avoid overloading at such small $\Delta\varepsilon_t/2$, the samples are designed to reach the set value of $\Delta\varepsilon_t/2$ in ~3000 cycles, which is a small life (~$0.4\%N_f$), relative to its fatigue-to-failure life (N_f). Both σ_{max} and $|\sigma_{min}|$ of GNG Cu during the whole fatigue test are larger than that (~88 MPa) of CG counterparts. Besides, GNG Cu exhibits a much longer fatigue-to-failure life (8.3×10^5 cycle) than that of CG Cu (2.1×10^5 cycle), which is consistent with the results reported under stress control [7].

An obvious tension-compression asymmetry with higher $|\sigma_{min}|$ than σ_{max} is detected in GNG Cu, although under symmetric tension–compression total strain amplitude control. At 3000 cycles, $|\sigma_{min}|$ of GNG Cu is 117 MPa while its σ_{max} is 96 MPa, showing a

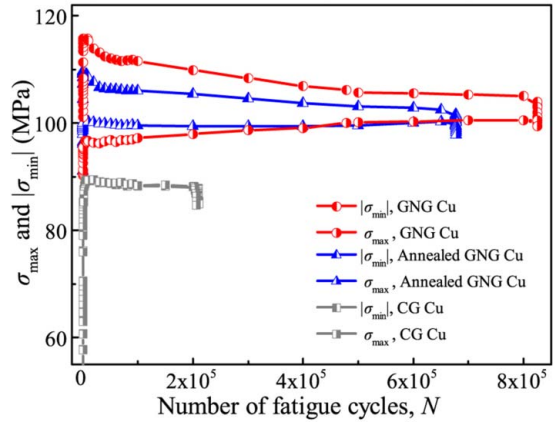

Figure 2. Cyclic stress (tensile maximum stress (σ_{max}) and compressive minimum stress (σ_{min})) responses of GNG Cu, annealed GNG Cu and CG Cu cyclically deformed at the total strain amplitude ($\Delta\varepsilon_t/2$) of 0.12%.

stress gap ($|\sigma_{min}|$-σ_{max}) as large as 21 MPa, which is fundamentally distinct from fully symmetric response of conventional face centre cubic CG metals reported in the literature [5,18,19]. Furthermore, $|\sigma_{min}|$ of GNG Cu gradually decreases with increasing cycles while its σ_{max} increases. Until at cycles before failure, $|\sigma_{min}|$ is still larger than that of σ_{max}, and the stress gap between them gets smaller (~3 MPa), suggesting that the degree of tension–compression asymmetry of GNG Cu gradually diminishes during cyclic deformation.

Figure 2 also shows that annealing treatment of GNG Cu can reduce tension–compression asymmetry. $|\sigma_{min}|$ of annealed GNG Cu at 3000 cycles is 111 MPa while its σ_{max} is 100 MPa at the same cycle, with a stress gap of 11 MPa, which is smaller than that of GNG Cu. With

increasing cycles, asymmetric response of annealed GNG Cu gradually recovers to quasi-symmetric response; stress gap ($\sim$1 MPa) almost disappears before failure. Note that both the stress level and fatigue-to-failure life (6.8×10^5cycle) of annealed GNG Cu are lower than that of GNG Cu, but still higher than that of CG counterparts.

The evolution of stress–strain hysteresis loops of GNG Cu (Figure 3(a)) and annealed Cu (Figure 3(b)) at $\Delta\varepsilon_t/2 = 0.12\%$ shows that besides inequality of tension-compression peak stress, their loops are also asymmetric, especially at initial cycles, quite different from that of CG Cu (Figure 3(c)). At 0.4%N_f, the maximum plastic strain amplitude of GNG Cu in the tension segment of hysteresis loop (Figure 3(a)) is 0.03%, much larger than that in the compression segment (0.01%), exhibiting a characteristic of asymmetry. With increasing cycles, hysteresis loops of both GNG Cu and annealed GNG Cu also gradually recover to be symmetric, like the trend of tension-compression peak stress.

Comparisons of fatigue results among GNG Cu, annealed CG Cu and CG Cu demonstrate that tension-compression asymmetry of GNG Cu is closely correlated with the microstructure of GNG layer. One prominent feature of GNG surface layer is characterized by high-density dislocations and curved GBs, similar to those observed in nanostructured metals prepared by severe plastic deformation [4]. Previous studies have shown that tension-compression asymmetry with a mean stress amplitude of 25–44 MPa is still detected in UFG Cu fatigued in strain-controlled low-cycle regime ($N_f < 10^5$ cycles) [20]. Tension-compression asymmetry is proposed to be an inherent phenomenon of nanostructured metals during fatigue.

It is accepted that the residual stress, associated with high-density defects, is readily developed in metals when straining, as a result of inhomogeneous plastic deformation in grains and/or between grains [14,21]. As shown in Figure 4(a), compressive residual stress in the surface layer of GNG Cu at the depth of 120 μm is 33 MPa and gradually increases at regions closer to the surface because a larger plastic strain is imposed during SMGT process. It reaches to a maximum value of 123 MPa at a depth of 40 μm but decreases to 89 MPa at the top surface, owing to the relaxation of the free surface. Annealing GNG Cu will partially release the residual stress to a smaller value (Figure 4(a)) and the maximum compressive residual stress in annealed GNG Cu decreases to 72 MPa at depth of 40 μm, which is consistent with its recovered microstructure (Figure 1(e,f)).

Residual stress in GNG Cu is also released during cyclic deformation, as shown in Figure 4(a) that the residual stress of GNG Cu sample at 40%N_f is almost the same as that of annealed GNG Cu. Furthermore, negligible residual stresses are detected in both GNG and annealed GNG Cu samples after fatigued to failure. Comparisons between the tension-compression asymmetry and residual stress state of GNG Cu and annealed CG Cu (Figures 2 and 4(a)) suggest that the tension-compression asymmetry of GNG Cu in strain-controlled fatigue tests is possibly induced by the residual stress in GNG layer.

Moreover, the gradually diminished trend of tension–compression asymmetry and residual stress in both types GNG Cu with increasing cycles suggests that they are mainly caused by microstructural evolutions in GNG layer. As shown in Figure 4(b,c), abnormally coarsed grain initiating from UFG subsurface layer and eventually extending to NG top surface is observed in both GNG and annealed GNG Cu sample fatigued at $\Delta\varepsilon_t/2$ of 0.12%, like that detected in fatigued GNG Cu under stress control [7].The abnormally coarsed grains in depth span 0–113 μm of annealed GNG Cu exhibit grain morphology and grain size distribution similar to that of GNG Cu. The abnormal coarsed grains, consuming surrounding UFGs and NGs with high-density defects, results in

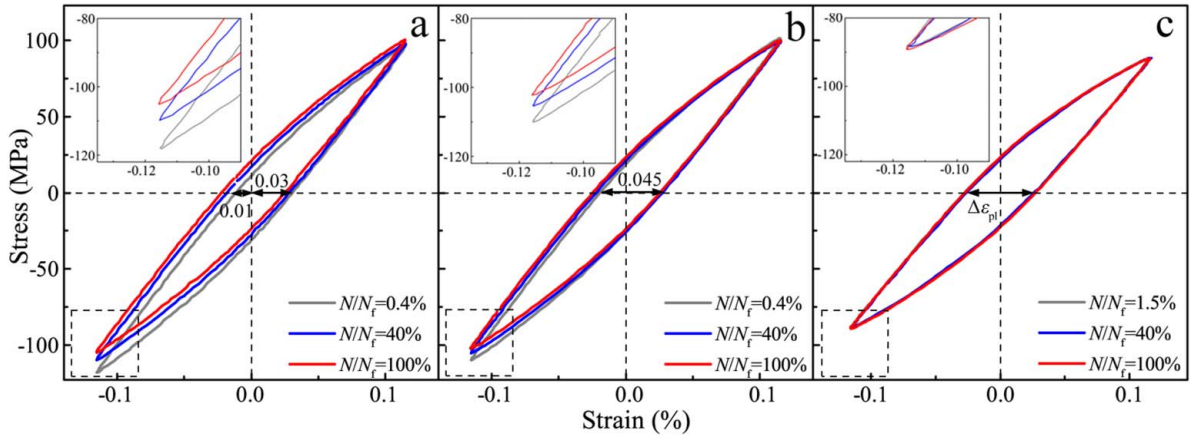

Figure 3. Variations of hysteresis loops of (a) GNG Cu, (b) annealed GNG Cu and (c) CG Cu cyclically deformed at $\Delta\varepsilon_t/2 = 0.12\%$.

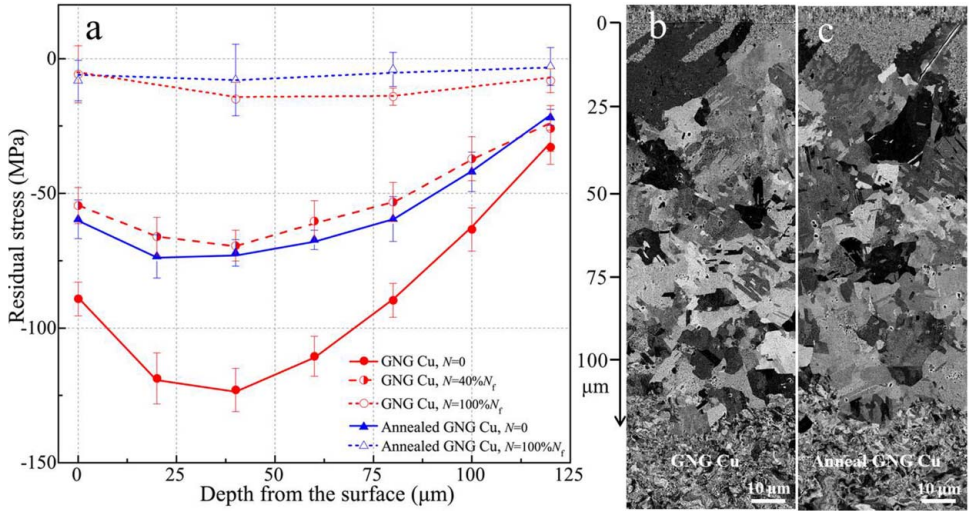

Figure 4. (a) In-depth residual stress distributions in GNG and annealed GNG Cu before, during (40% N_f) and after fatigue-to-failure (100% N_f). Typical cross-sectional SEM images of microstructure of (b) GNG Cu and (c) annealed GNG Cu after fatigue-to-failure, showing that abnormal grain coarsening phenomenon is observed in both samples.

the relaxation of residual stress in GNG layer and gradual disappearance of asymmetric response of both GNG Cu after fatigued to failure.

The presence of compressive residual stress in GNG layer implies that it is in a state of compressive residual strain [21–23]. When the sample is deformed in tension during fatigue tests, the residual compressive stress in GNG layer will counteract part of stress increment, thus resulting in a decreased σ_{max} of GNG/CG Cu, relative to the counterparts without any residual stresses. In contrast, when the sample is deformed in compression, an increased σ_{min} is obtained as a result of superposition of both internal residual compressive strain and imposed compressive cyclic strain. Thus, the compressive residual stress in GNG layer leads to an obvious tension-compression asymmetry of GNG Cu with larger σ_{min} than σ_{max}. A higher residual stress in GNG layer contributes to a more significant cyclic asymmetry, as shown in Figure 2.

Previous studies showed that a large long-range back stress will be developed in GNG metals during tensile testing, owing to the inhomogeneous plastic deformation of the GNG layer with gradient distribution of grain size and strength [2,24]. However, in this study, the estimated back stress in both tension and compression segments of GNG Cu at initial cycles, according to the classic Dickson method [25–27], are very small and nearly comparable with that of CG counterpart, possibly owing to the GNG layer still mainly undergoing an elastic deformation at such small $\Delta\varepsilon_t/2$, and negligible microstructural changes in each cycle [25–27]. Thus, the above analysis based on experimental results (Figures 1–4) demonstrates that the observed tension-compression asymmetry in fatigued GNG Cu is mainly induced by compressive residual stress.

GNG Cu exhibits a relatively longer fatigue life (8.3×10^5 cycle) than that of annealed GNG Cu (6.8×10^5 cycle) (Figure 2). Considering the value of residual stress in these two type of GNG Cu, we would point out that the existence of residual compressive stress in the GNG layer exhibits a positive effect on enhancing high-cycle fatigue life of GNG Cu. On one hand, although cyclically loading under the same $\Delta\varepsilon_t/2$, GNG Cu with a larger residual stress exhibits a relatively smaller plastic strain range ($\Delta\varepsilon_{pl}$) than that of annealed GNG Cu, especially at initial cycles, owing to the residual stress induced change of hysteresis loop (Figure 3). As shown in Figure 3(a), $\Delta\varepsilon_{pl}$ of GNG Cu at 0.4% N_f is 0.04%, which is smaller than that (0.045%) of annealed GNG Cu (Figure 3(b)). This will lead to the relatively slower plastic strain accumulation and retardation of fatigue crack initiation in GNG Cu. On the other hand, the residual compressive stress itself can also benefit for suppressing fatigue crack initiation, by changing the local stress states [5].

4. Conclusion

In this work, through utilizing strain-controlled high-cycle fatigue tests, we investigate the cyclic stress response of two GNG Cu samples with different residual stresses. Obvious tension-compression asymmetry with compressive minimum stress higher than tensile maximum stress is observed in GNG Cu cyclically deformed at $\Delta\varepsilon_t/2 = 0.12\%$. With increasing cycles or annealing at low temperature, the degree of tension–compression

asymmetry of GNG Cu gradually diminishes. The observed tension-compression asymmetry of GNG Cu is mainly caused by the residual compressive stress in the GNG layer during SMGT. The presence of residual compressive stress also contributes to an enhanced high-cycle fatigue life of GNG Cu.

Acknowledgements

The authors are grateful to Mr X. Si for assistance in sample preparation.

Disclosure statement

No potential conflict of interest was reported by the authors.

Funding

L.L. acknowledges the financial support by the National Science Foundation of China [grant nos. 51471172, 51420105001 and U1608257] and the key Research program of Frontier Science, CAS.

References

[1] Fang TH, Li WL, Tao NR, et al. Revealing extraordinary intrinsic tensile plasticity in gradient nano-grained copper. Science. 2011;331:1587–1590.
[2] Wu XL, Jiang P, Chen L, et al. Extraordinary strain hardening by gradient structure. Proc Natl Acad Sci USA. 2014;111:7197–7201.
[3] Wei Y, Li Y, Zhu L, et al. Evading the strength-ductility trade-off dilemma in steel through gradient hierarchical nanotwins. Nat Commun. 2014;5:3580.
[4] Chen W, You ZS, Tao NR, et al. Mechanically-induced grain coarsening in gradient nano-grained copper. Acta Mater. 2017;125:255–264.
[5] Suresh S. Fatigue of materials. 2nd ed Cambridge: Cambridge University Press; 1998.
[6] Roland T, Retraint D, Lu K, et al. Fatigue life improvement through surface nanostructuring of stainless steel by means of surface mechanical attrition treatment. Scripta Mater. 2006;54:1949–1954.
[7] Yang L, Tao NR, Lu K, et al. Enhanced fatigue resistance of Cu with a gradient nanograined surface layer. Scripta Mater. 2013;68:801–804.
[8] Huang HW, Wang ZB, Lu J, et al. Fatigue behaviors of AISI 316L stainless steel with a gradient nanostructured surface layer. Acta Mater. 2015;87:150–160.
[9] Long JZ, Pan QS, Tao NR, et al. Abnormal grain coarsening in cyclically deformed gradient nanograined Cu. Scripta Mater. 2018;145:99–103.
[10] Altenberger I, Scholtes B, Martin U, et al. Cyclic deformation and near surface microstructures of shot peened or deep rolled austenitic stainless steel AISI 304. Mater Sci Eng A. 1999;264:1–16.
[11] Wagner L. Mechanical surface treatments on titanium, aluminum and magnesium alloys. Mater Sci Eng A. 1999;263:210–216.
[12] Villegas JC, Shaw LL, Dai K, et al. Enhanced fatigue resistance of a nickel-based hastelloy induced by a surface nanocrystallization and hardening process. Philos Mag Lett. 2005;85:427–438.
[13] Nikitin I, Altenberger I. Comparison of the fatigue behavior and residual stress stability of laser-shock peened and deep rolled austenitic stainless steel AISI 304 in the temperature range 25-600 degrees C. Mater Sci Eng A. 2007;465:176–182.
[14] Meyers MA, Chawla KK. Mechanical behavior of materials. 2nd ed. Cambridge: Cambridge University Press; 2009.
[15] Mughrabi H, Höppel HW. Cyclic deformation and fatigue properties of very fine-grained metals and alloys. Int J Fatigue. 2010;32:1413–1427.
[16] Cullity BD. Elements of X-Ray Diffraction. 2nd ed. Reading (MA): Addison-Wesley; 1978.
[17] Withers PJ, Bhadeshia HKDH. Overview—Residual stress part 1—Measurement techniques. Mater Sci Technol. 2001;17:355–365.
[18] Rasmussen KV, Pedersen OB. Fatigue of copper polycrystals at low plastic strain amplitudes. Acta Metall. 1980;28:1467–1478.
[19] Winter AT. Model for fatigue of copper at low plastic strain amplitudes. Philos Mag. 1974;30:719–738.
[20] Höppel HW, Brunnbauer M, Mughrabi H. Cyclic deformation behaviour of ultrafine-grained size copper produced by equal channel angular pressing. In: Werkstoffwoche-Partnerschaft, editor. Proceedings of materials week 2000. 2000 Sep 25–28; Frankfurt, 2000. p. 1–8.
[21] Orowan E. Causes and effects of internal stresses. In: Rassweiler GM, Grube WL, editor. Internal stresses and fatigue in metals. NewYork (NY): Elsevier; 1959. p. 59–80.
[22] Kwofie S. Description and simulation of cyclic stress-strain response during residual stress relaxation under cyclic load. Proc Eng. 2011;10:293–298.
[23] Wang Q, Liu X, Yan Z, et al. On the mechanism of residual stresses relaxation in welded joints under cyclic loading. Int J Fatigue. 2017;105:43–59.
[24] Wu X, Zhu Y. Heterogeneous materials: a new class of materials with unprecedented mechanical properties. Mater Res Lett. 2017;5:527–532.
[25] Mughrabi H. On the current understanding of strain gradient plasticity. Mater Sci Eng A. 2004;387-389:209–213.
[26] Kuhlmann-Wilsdorf D, Laird C. Dislocation behavior in fatigue II. Friction stress and back stress as inferred from an analysis of hysteresis loops. Mater Sci Eng. 1979;37:111–120.
[27] Dickson JI, Boutin J, Handfield L. A comparison of 2 simple methods for measuring cyclic internal and effective stresses. Mater Sci Eng. 1984;64:L7–L11.